Dalton Transactions

An HASApf-Redoxin Complex causing Asymmetric Catalytic Oxidation via the Regenerative Formation of a Reactive Oxygen Species

Journal:	*Dalton Transactions*
Manuscript ID:	DT-ART-05-2015-001768.R1
Article Type:	Paper
Date Submitted by the Author:	09-Jun-2015
Complete List of Authors:	Nagaoka, Hiroyuki; Sanyo Foods. Co., Ltd, R & D

An HASApf-Redoxin Complex causing Asymmetric Catalytic Oxidation via the Regenerative Formation of a Reactive Oxygen Species

*Hiroyuki Nagaoka**

Sanyo Shokuhin Co., Ltd. R & D, 555-4 Asakura, Maebashi, Gunma 371-0811, Japan

E-mail: hnagaoka@sanyofoods.co.jp, Tel: +81-27-220-3471, Fax: +81-27-220-3477

Abbreviations: HASApf: heme acquisition system A from *Pseudomonas fluorescens* Pf-5, ME: membrane-bound enzymes, PP: pea protein, DMSO: dimethyl sulfoxide, PP-gel: calcium-alginate gel containing PP, GA: glutaraldehyde, CMME: compound-modified ME, AGME: PEG (MW: 4000/1000 = 1/2)-aggregated ME, *S*-**1**: *S*-(+)-1-(6-methoxynaphthalen-2-yl)ethanol, *S*-**2**: *S*-(+)-1-(2-naphthyl)ethanol, ICP-AES: inductively coupled plasma-atomic emission spectroscopy, IC: ion chromatography. ESR: electron spin resonance, FTIR: Fourier-transform infrared spectroscopy.

Graphical abstract:

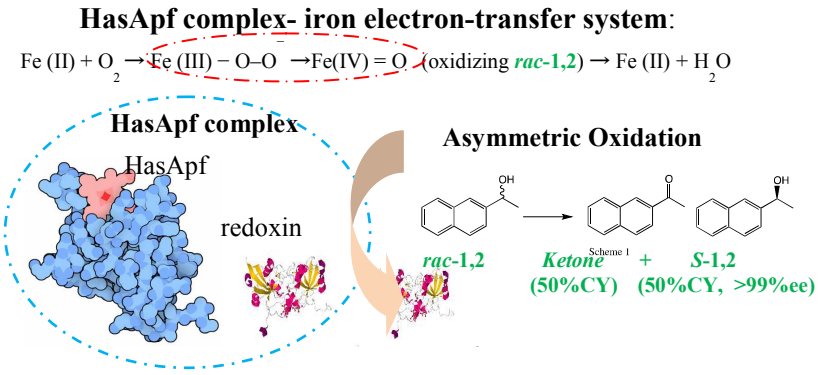

Abstract: A PP-HASApf-redoxin complex eluted from encapsulated PP gel with aeration displays asymmetric oxidation activity over 200 times greater than that of a similar protein expressed by E. coli cells. The intermediate spin, identified in the ESR spectrum, appears at g = 4.3 and g = 2.0, suggesting that the iron electron-transfer system for the asymmetric oxidation of secondary alcohols may be successfully created by the PP-HASApf-redoxin complex (39 kDa). FTIR experiments provided values $\nu_s(SO_2) \approx 950–1050$ cm^{-1} and $\nu_{as}(SO_2) \approx 1100–1200$ cm^{-1} for metal-bound sulfinate S–O and Fe–O vibrations. The sulfur and iron detected by physicochemical inspection (IC/ICP-AES) may facilitate the electron transport of a sulfate-iron complex (e.g., rubredoxin (6 kDa) or ferredoxin (9 kDa)) to the HASApf (21 kDa). The observations are consistently acceptable; i.e., the oxygen-driven PP-HASApf-redoxin complex functions regenerate via the successive asymmetric catalytic event– Fe(II) + O_2 → Fe(III) − O–O^- → Fe(IV) = O (oxidizing *rac*-1 or *rac*-2) → Fe(II) + H_2O. Therefore, the use of a raw biomaterial as a PP-HASApf-redoxin complex-catalytic system for asymmetric oxidation is an important novelty, despite the apparent difficulties in working with pure dehydrogenase enzymatic/redox-cofactor systems for biotransformation.

Introduction

An enantioselective catalytic system that promotes the formation of versatile chiral building blocks, fine chemicals, pharmaceuticals, flavors, and biologically active molecules is reported herein. However, there are limitations associated with its application to microbial synthesis.[1] A review covering the well-known alcohol dehydrogenase enzyme system that incorporates redox cysteine disulfide bonds, redox zinc, and a redox cofactor has already been published,[2] and the high cost and instability of the redox cofactors in enzymatic synthesis justifies the efforts to regenerate them.[3] However, the use of a porphyrin/Fe holoprotein (e.g., HASA) incorporating an iron electron-transfer system for the asymmetric oxidation (with oxygen) of secondary alcohols in organic synthesis has not yet been examined,[4] although it is generally accepted that the system of hemophore HasA secreted by host ABC transporters[5] enables

heme uptake across the cell outer membrane and spontaneously transforms it into the HasR receptor at the heme-binding site.[6] Thus, the use of a hemophore HASA system counteracts the apparent difficulties in working with pure dehydrogenase enzymatic/redox-cofactor systems for microbial biotransformation.[7]

In the past decade, the use of biomaterials as plant catalytic systems incorporating redox cofactors for asymmetric oxidation reactions has been investigated.[8] In particular, the redox protein eluted from PP encapsulated with calcium alginate gel (PP gel) is available for synthesis[9] and the enantiomeric resolution of *m*- and *p*-substituted racemic aryl methyl carbinols.[9b] Besides proteins, other biomaterials used for this purpose include young wheat or barley leaves, wheat bran, *Artemisia vulgaris* L. var. *A. indica*, carrots, and pumpkins.[9d] Specifically, ME are activated by a buffered glycine reaction solution (pH 9.0–10.0).[10] Eluted from encapsulated PP, under aeration, ME can be applied to turnover kinetic resolutions (Equation 1); e.g., ME may synthesize *S*-(+)-**1** (*S*-naproxen precursor)[11] utilizing a GA/a PEG (4000)-coated ME.[12] In addition, an iron electron-transfer system may be incorporated as an oxygen-driven catalytic system for asymmetric oxidation.[13] The species' exact nature engaged in the key reaction is demonstrated to be consistent with that of a heme-binding protein (i.e., HBP).[12] An N-terminal sequence comparison[12,13] also provides 93% similarity with a 20.853 kDa hemophore HASApf gene product [*Pseudomonas fluorescens* Pf-5].[14] Therefore, these features are regenerated by successive asymmetric catalytic events using an incorporated iron electron-transfer system in the presence of oxygen. This process is similar to that utilized by the oxygen-driven cytochrome P450: cysteine–Fe(II) + O_2 → Fe(III)–O–O^- → Fe(IV) = O (oxidizing *rac*-1 or *rac*-2) → Fe(II) + H_2O.[15] However, an HASApf gene would be identified through the application of asymmetric oxidation, because no BLAST-hit data exemplifying the gene was determined in the previous process due to the broad acquisition by PP.[12] In this study, evidence is provided to support the fact that porphyrin/Fe holoprotein (e.g., cytochrome P450[16] or HASA[5]), among the used PP, is the actual catalyst. Considering the possible formation of sulfate, a hypothesis is tested whether its formation leads to the presence of heme, which is coordinated by thiolate.[17,18]

Experiments conducted using ESR spectroscopy, FTIR, and isotopic analytical methods require the assignment of a redox protein. This study aims to (1) demonstrate the asymmetric oxidation activity of an HASApf expressed by bacteria, (2) characterize an HASApf-redoxin complex eluted from PP using the ESR and FTIR analyses, and (3) present an HASApf-redoxin complex as a new asymmetric oxidation catalysis tool similar to that utilized by the oxygen-driven cytochrome P450.[16]

[**Equation 1**]

Results and Discussion

Kinetic resolutions of bacterial HasApf and each fraction eluted from PP gel

The broad acquisition by PP, rather than by bacterial contamination, is exemplified in Scheme 1. *Pseudomonas fluorescens* Pf-5 is absent in the PP analysis for common bacteria (CFU/g), whereas aerobic spore-bearing bacteria (*Geobacillus, Alicyclobacillus, Bacillus, Paenibacillus*) and catalase-positive and gram-positive coccus (*Staphylococcus, Kocuria, Micrococcus*) are detected. The time course of the asymmetric oxidation activity with a HasApf purified from *P. fluorescens* Pf-5 (20 μM) utilizing substrate *rac*-2 (0.8 mM) in highly bubbled oxygen water as a solvent (5.0 mL) is summarized in Figure 1; monitoring *S*-2, *R*-2, and product ketone. These results indicate that the asymmetric oxidation activities of each fraction occur in the PP-HASApf-redoxin complex eluted from PP gel due to the broad acquisition by PP (Table S1)[12,13]. A redox protein obtained from an HASApf expressed can oxidize an enantiomer in *rac*-2; thus, the other enantiomer could be obtained with high enantioselectivity (i.e., 50% yield, 99% ee; Figure 1) although the asymmetric oxidation activity of PP-HAS-Apf-redoxin complex (0.1 μM, which is equal to PEG-precipitate 2 (30 mg); Table 2), is over 200 times greater than that of the HASApf expressed (20 μM), suggesting that a nonplanar PP-HASApf-redoxin complex and/or oxoferryl-Fe(IV) = O may be formed during oxidation between 0 h and 40 h incubations (Figure 1). Therefore, the PP-HASApf-redoxin complex from PP gel under aeration may be useful for catalyzing secondary metabolites resistant to the toxic effects of antibiotics in the presence of oxygen.

[Scheme 1 and Figure 1]

Inductively coupled plasma-atomic emission spectrometry (ICP-AES) and elemental analysis (IC)

ICP-AES and IC analyses of dried supernatant 2 and dried HASApf expressed (*P. fluorescens*) show that if iron (Fe) and sulfur (S) in dried supernatant 2 are reduced by half, the oxygen becomes higher compared with that of HasApf, allowing us to detect a trace of the coordination of Fe ions and suggesting that a sulfate heme may be effectively purified (Table 1). The results also suggest that either an iron–sulfur cluster may be effectively purified in their electron transfer chain or a sulfate (ion) heme may be created because of the existence of iron (Fe) and sulfur (S) (Table 1). In previous experiments,[12,13] a PP-HASApf single-band (S/Fe ratio = 3; only 33 out of 204 residues) was utilized in combination with the gel filtration process, despite its molecular mass being 20.8 kDa (Figures 1S and 2S); the full length gene sequence may be partly replaced by a cysteine sulfate-iron complex due to the broad acquisition by pea (Table 3). This activity increases when using a 100 nm oxygen bubble-water (Dissolved oxygen (DO): 8.0 ± 0.5 mg/L, Unit of activity: 0.7 ± 0.02 mU) instead of distilled water (DO: 7.5 ± 0.5 mg/L, Unit of activity: 0.6 ± 0.02 mU), suggesting that an incorporated iron electron-transfer system may be activated by highly bubbled oxygen water (Table 2). The results also suggest that either an iron–sulfur cluster is effectively purified in their electron transfer chain or a sulfate (ion) heme may be created because of the presence of Fe and S (Table 1), as well as oxygen-driven cytochrome P450.[7,16]

[Tables 1, 2, and 3]

SDS-PAGE analysis confirms cysteine thiolate coordination to the heme

SDS-PAGE was performed on (A) supernatant 1 (10 μL), (B) supernatant 2 (10 μL), (C) supernatant 2 after ultrafiltrating with Vivaspin 2–10 K (10 μL), and (D) sample C extracted by hexane after the reaction. The results suggest that PP-HASApf (P-21, bands 2) is obtained because of the separation of a redoxin from the PP-HASApf-redoxin complex (P-39, bands 1) (Figures 2, S1, and S2). Furthermore, the filtration of supernatant 2 (lane B, mixture of proteines) by Vivaspin (MWCO 10kD), a protein sample concentrator, surprisingly yields a single P-39, suggesting that P-39 can be effectively

filtrated via the different water solubility of MEs eluted/purified in PP gel under aeration.[12,13] Moreover, P-21 is similar to an HASApf expressed because of its appearance at 20.8 kDa and query coverage of >93% when S/Fe ratio is 3 (only 33 out of 204 residues; Table 3).[12,13] Thus, the PP-HASApf gene originates not from the PP (*Pisum sativum*) but from the commensal bacteria *P. fluorescens* Pf-5.[17] It is therefore hypothesized that at P-39, P-21 is realized through an iron–sulfur cluster aggregation (e.g., rubredoxin (18 kda; 6 kDa × 3); Table 3) for an electron transfer partner: NADPH → FAD-containing reductase → iron–sulfur complex (e.g., ferredoxi ≒18 kda; 9 kDa × 2) → P450).[15,22] These observations are consistent in the presence of iron (Fe), sulfur (S), and oxygen (higher 39 wt%) in dried supernatant 2 (Table 1).

[Figure 2]

FTIR analysis confirms cysteine thiolate coordination to the heme

The supernatant 2 dried FTIR spectrum confirms the existence of a thiolate coordination structure in the PP-HasA structure for controlling the large number of bands for proteins in the range 950–1250 cm^{-1}, as previously reported (Figures 3 and S3).[12,13] This is supported by the consistency between FTIR (Figure 3) and elemental analysis results (Table 1). There are differences between the FTIR spectra of dried HasApf (lower at 950–1250 cm^{-1}) and dried supernatant 2 after ultrafiltering with Vivaspin 2–10 K (higher at 950–1250 cm^{-1}): a reactive oxygen species (Fe(III)–O–O^- → Fe(IV) = O) promotes the appearance of a sulfate (S–O: a superoxoiron–cysteinate) in the range 950–1250 cm^{-1} (Figure 3). The peak $\nu_s(SO_2)$ ≈ 950–1050 cm^{-1} or $\nu_{as}(SO_2)$ ≈ 1100–1200 cm^{-1} may be attributed to a metal-bound sulfinate S–O and Fe–O vibrations.[18] PP gel oxygen absorption occurs under aeration. Instead of an iron–sulfur cluster, cysteine thiolate may be coordinated to the heme with cysteines identified in 33 residues (Table 3), leading to the formation of a reactive oxygen species via an iron electron-transfer system (cysteine–Fe(II) + O_2 → Fe(III)–O–O^- → Fe(IV) = O (oxidizing *rac*-1 or *rac*-2) → Fe(II) + H_2O), which results in water solubility (PP → ME including a PP-HASApf-redoxin complex). The formation

of sulfate through the oxidation of a thiolate ligand is based on a model complex that includes thiolate ligation (non-heme)[18] and Fe(IV) = O as the active intermediate (Figure 3). ESR analysis provides evidence for the principal Fe(IV) = O.[19]

[Figure 3]

ESR analysis of supernatant 2 after ultrafiltration

The asymmetric oxidation of dried supernatant 2 eluted from PP gel can be activated by the formation of a reactive oxygen species in the signals for g = 4.3 and g = 2 (Figure 4a), suggesting that the ferric form (PP-HASApf-ferrodoxin or –rubredoxin complex) and or oxoferryl-Fe(IV) = O) (Figure 4). ESR analysis suggests that the intermediate spin (S = 3/2: Fe(IV) = O) via an iron electron-transfer system occurs in the presence of oxygen. This is also supported by the consistency of the ESR iron spectrum due to the promotion of a reactive oxygen species (Fe(III)–O–O^{-}), leading to the appearance of higher spin singles (Fe(IV) = O) oxidizing *rac*-1 or *rac*-2 (Figure 3).[18] The spin iron heme(III) porphyrin complexes switch the ground state, generating a crossover triangle: i.e., high spin (S = 5/2; g = 6) and low spin (S = 1/2; g = 2) in fellic-Fe(III), and intermediate spin (S = 5/2 and 3/2; g = 4.3) in oxoferryl-Fe(IV) = O or -Fe(V) = O.[19] Therefore, the evidence for the principal involvement of Fe(IV) = O was confirmed by the decrease of the high spin signal (g = 6 → g = 4.3 and 2);[20] the catalytic cycle between Fe(II) heme and Fe(IV) = O heme has never been reported.[19] The PP-HASApf-redoxin complex eluted from PP gel may catalyze secondary metabolites in the presence of oxygen, a process similar to that utilized by the oxygen-driven cytochrome P450.[7,16]

[Figure 4]

There is an interesting phenomenon in the broad acquisition of HASApf gene [*Pseudomonas fluorescens* Pf-5] by the pea plant (PP). Some gram-negative bacteria such as *Pseudomonas aeruginosa* and *Yersinia pseudotuberculosis* have developed a siderophore system[5] and, under iron-limiting conditions, they transport chelate-iron to the bacteria therein by utilizing the hemophore HASA. The *P.*

fluorescens Pf-5 (a gram-negative bacterium) is a rhizobacterium and widely utilized by agriculture (e.g., pea) as it prevents plant diseases and promotes growth.[17] Therefore, the fluorescent Pf-5 is able to colonize plant roots as well as an endosymbiosis such as chloroplast/mitochondria[21] and then suppress soilborne pathogens.[14] Therefore, the PP-HASApf gene from the PP colonized by *P. fluorescens* Pf-5 may be recreated by a new regenerative system via a cystein thiolate coordinated to heme in a mechanism resembling that applied for the oxygen-driven cytochrome P450: cysteine–Fe(II) + O_2 → Fe(III)-O-O^- → Fe(IV) = O (oxidizing *rac*-1 or *rac*-2) → Fe(II) + H_2O.[15] The observed non-heme iron ESR signals (g = 4.3) result from the PP-HASApf-redoxin complex that was formed and/or oxoferryl-Fe(IV) = O by the formation of sulfate through thiolate ligand oxidation in the process of PP gel aeration (higher 39 wt%; Table 1). On the other hand, the HASApf expressed appears to include a small amount of sulfate–iron residue from E. coli cells (Table 1) and is able to be weakly activated in highly bubbled oxygen water as a solvent (Figure 1), suggesting that an HASApf-redoxin complex may be recreated in a reaction tube without any cap (Figure 1)[5] while His/Tyr-heme remains in the six-coordinate low-spin state (Figure 4).[5] Therefore, it is postulated that an incorporated rubredoxin and/or ferredoxin may have caused the higher asymmetric oxidation activity in the promotions of both an HASApf-redoxin complex (Figure 4) and a reactive oxygen species (oxoferryl-Fe(IV) = O) (Figure 3) to form the iron catalytic center. Although cytochrome P450 electron-transport chains corresponding to NADPH → FAD-containing reductase → iron-sulfur complex → P450 have been reported,[22] the present study provides preliminary evidence for iron–sulfate participating in the HASApf-redoxin complex.

Consequently, this process would enable to overcome the apparent difficulties in working with pure dehydrogenase enzymatic/redox-cofactor systems for biotransformation. Herein, a new method for the purification of the PP-HASApf-redoxin complex is clarified, and the use of a raw biomaterial as an HASApf-redoxin complex catalytic system is proposed for heterogeneous enzyme catalysis,[23] incorporating a redox cofactor to perform asymmetric oxidation. In the future, biomaterials containing the HASApf-redoxin complex are expected to become important as not only foods but also biological

catalysts for the synthesis of optically active alcohols using environmentally friendly systems that promote industrial sustainability.

Materials and methods

Inductively coupled plasma-atomic emission spectrometry and elemental analysis

Metal content measurements were obtained through ICP-AES (Shimadzu, ICPS-7500). The protein powder (0.5 g) was added to a solution of purified water (50 mL) and 60% HNO_3 (Kokusan, 10 mL) in a 100 mL beaker. The mixture was digested through heating on a hot plate for 1 h. The digested sample was diluted to 50 mL with purified water, and the metal content was then measured. Elemental analysis of the samples (2 mg) was performed on a Perkin-Elmer PE 2400 Series II analyzer and a type "vario EL cube" analyzer (Elementar Co., Ltd).

Preparation of AG-Precipitate 2, PEG-Precipitate 2, and dried Supernatant 2.

PP (10 g) was added to 200 mL aqueous sodium alginate 0.75% and encapsulated with $CaCl_2$ (500 mL, 39 g/L). The PP gel was air-exposed for 5 h, and the resulting HasA suspension was extracted at 40 °C with distilled water (200 mL) in a 500 mL Erlenmeyer flask through centrifugation at 150 rpm for over 40 h. In order to produce AG-precipitate 2, the precipitate 1 (wet: 16 g) was centrifuged (at 10,000 rpm for 10 min), then dissolved in a 5% (v/v) PEG (MW: 1000/4000 = 2/1)/50 mM glycine–NaOH solution (pH 9.0, 100 mL), and stored for over 20 h to allow aggregation. After storing, the precipitate was freeze-dried under vacuum and crushed using a ball mill. PEG-precipitate 2 was produced as follows: the precipitate 1 (wet: 16 g) was dissolved in a 50 mM glycine–NaOH solution (pH 9.0, 100 mL), with the adddition of PEG (MW 4000) (500 mg) and a 25% (v/v) aqueous glutaraldehyde (GA) solution (2 mL) to obtain an overall 0.5% (v/v) GA solution for cross-linking, which had a duration over 3 h. Finally, to produce the dried supernatant 2, the precipitate 1 (wet: 16 g) was dissolved in a 50 mM glycine–NaOH solution (pH 9.0, 100 mL) for over 3 h, and the mixture was centrifuged at 10,000 rpm for 10 min. The resulting supernatant 2, ultra-filtered with Vivaspin 2–10 K, was freeze-dried under

vacuum, dried at over 50 °C on a hot plate (As One: THI-1000) [–50 °C/10 Pa (1 h) → 5 °C/min → +50° C/10 Pa (22 h)], and crushed using a ball mill.

General procedure for reactions using each PP gel fraction

Rac-1 (1000 mg) was dissolved in DMSO as a cosolvent (50 mL). The substrate solution (30 μL, 20,000 ppm) and each fraction (precipitate-dried samples for 30 mg, suspension samples for 5 ml) were combined in an 18 mm × 15 mL test tube, adding distilled water (4.0 mL for precipitate-dried), and the reactions were performed at 40°C with magnetic stirring at 700 rpm. Subsequently, the reaction mixture was centrifuged at 3500 rpm (5 min) and then extracted by adding n-hexane (4.0 mL). The ee was calculated for *rac*-1 (0.8 mM or 1.2 mM) or *rac*-2 (0.8 mM or 1.2 mM), which were separated using a Daicel Chiralcel OB-H column ((S)-isomer/(R)-isomer/product ketone = 7.8/8.8/11.6 min) or a Daicel Chiralpak AS-H column ((R)-isomer/(S)-isomer/product ketone = 7.5/8.25/9.5 min) connected to a HPLC LC-10A system (Shimadzu). The analytical conditions were as follows: mobile phase, n-hexane/IPA: 9/1, flow rate: 1.0 mL/min, temperature: 30 °C, wavelength: UV 254 nm. The stereochemistry of the isolated optically active alcohol was identified, as reported in previous studies by comparing the specific rotation values (+ or −) obtained using a polarimeter.

SDS-PAGE of each fraction eluted from PP gel

Each sample, supernatant 1 (A) (10 μL), supernatant 2 (B) (10 μL), supernatant 2 ultra-filtrated (C) (10 μL), and sample C extracted by hexane (D) (10 μL) were heated to 100 °C (5 min) after mixing with 2 × SDS sample buffers (Sigma-Aldrich) and electrophoresing with a molecular marker (Bio-rad) in a buffer (Tris–HCl (25 mM) and glycine (0.91 M), 0.1% SDS, pH 8.3) using a SDS-PAGE mini system (TEFCO). After completion, the gel was stained with CBB (PhastGel Blue R, Amersham Bioscience).

FTIR and ESR analyses of dried supernatant 2

FTIR analysis was performed using a portable ATR instrument (A2 Technologies, ML version) (Figure 1). A single-bounce internal reflection method with a diamond crystal was applied to obtain the

spectra of a dried supernatant 2. To ensure uniform contact, the dried supernatant 2 sample was pressed on the diamond crystal by a pressure device attached to the ML FTIR instrument. ESR analysis was performed using a JES-FA200 type (Japan Electron Optics Laboratory Co., Ltd.), operating in the following conditions: magnetic field: 322.5 ± 250 mT, modulation field: 0.6 mT, time constant: 0.3 s, microwave power: 1 mW, sweep time: 8 min, and temperature: −165 °C. Although usually water significantly interferes with the FTIR spectra of biological samples, no water band is observed in the present chart (Figure 3), because the supernatant 2 was effectively prepared to a dried form for this analysis. Indeed, supernatant 2 may be purified by ultra-filtration alone.

N-terminal amino acid sequence and BLAST analysis of single band 2 in sample D

Precise analysis of the N-terminal amino acid sequence (protein sequencing) of the single band 2 in sample D obtained via SDS-PAGE was accomplished using the PPSQ-21A protein sequencer (Shimadzu). This method removes the amino acids from the protein or peptide N-terminal one by one (Edman degradation method). The amino acid sequence was determined from the HPLC retention times (chromatograms) with UV detection. Blotting was achieved at a constant voltage (25 V) for 1 h using Fluorotrans membrane (Pall), NuPAGE transfer buffer (Invitrogen), CBB-R250 (BIO-RAD), and 50% methanol with 5% acetic acid; the polyvinylidene difluoride membrane targeted band (near 20 kDa) was also measured. To acquire the amino acid sequence, local similarity regions between the sequences were identified using BLAST.

HasApf protein expression and purification

The HASApf coding sequence was amplified by a polymerase chain reaction with bacterial genomic DNA (*P. fluorescens*) and cloned into pQE-30 (Qiagen; Tokyo Japan) using the BamHI and HindIII restriction sites. The resultant plasmids were transformed into M15 *E. coli* cells, and the transformants were cultured through continuous shaking at 30 °C in terrific broth, adding 50 μL/mL ampicillin. At OD_{600} = 1, 0.1 mM isopropyl β-D-1-thiogalactopyranoside was added, followed by incubation at 30 °C for an additional 16 h. The harvested cells were resuspended in 15 mM potassium phosphate, including 1

mM EDTA and 2 mM 2-mercaptoethanol. The cells were lysed by sonication, and the HasA proteins were purified from the supernatant, using a His-Tag purification column. Further purification was performed using a Sephadex G-75 gel filtration column (GE Healthcare Japan Corp.) or a Mono Q anion-exchanger column (GE Healthcare Japan Corp.) whenever necessary. The wild type proteins were purified to the heme-loaded holoforms.

Conclusions

The scope of this study is to clarify all the species engaged in the heterogeneous biocatalytic oxidation sequence, including the process regarding the PP-HASApf-redoxin complex eluted from encapsulated PP under aeration. The ESR spectrum appears at the g = 4.3 and g = 2.0 signals because of the intermediate spin (S = 5/2 and 3/2) in sulfate-iron complex (a redoxin) and/or oxoferryl-Fe(IV) = O. Furthermore, FTIR experiments provide values between 950 to 1250 cm^{-1} because of metal-bound sulfinate S–O and Fe–O vibrations. This indicates that the PP-HASApf may be coordinated to a redoxin, not His/Tyr, and suggests that it can perform successive asymmetric catalytic events via an incorporated iron electron-transfer system, with highly bubbled oxygen water as a solvent. The asymmetric oxidation activity is attributed to an HASApf-redoxin complex that is native to the commensal bacteria *P. fluorescens* Pf-5 due to the broad acquisition by the plant (e.g., PP). The use of a raw biomaterial as an HASApf-redoxin complex catalytic system for asymmetric oxidation is a novelty, which overcomes the apparent difficulties in working with pure dehydrogenase enzymatic/redox-cofactor systems for biotransformation.

Acknowledgments: The author would like to thank Associate Prof. Osami Shoji from Nagoya University and Prof. Shin-ichi Ozaki from Yamaguchi University for providing the HASApf sample. Thanks is also due to General Manager Koh Ueda from Wako Pure Chemical Industries Ltd., for placing SanCat-*R* on the market (PEG precipitate 2: Code No. 351-34213 (5 g)). This study was fully funded by

Sanyo Shokuhin Co., Ltd.

Electronic supplementary information (ESI) available: Description of the material (SI Figure S1–S3, and Table S1) is available via the Internet at http://pubs.rsc.org/.

References

1 (a) H. E. Schoemaker, D. Mink and M. G. Wubbolts, *Science* 2003, **299**, 1694. (b) M. Kamezawa, M. Kitamura, H. Nagaoka, H. Tachibana, T. Ohtani and Y. Naoshima, *Liebige Ann.* 1996, **1996**, 167.

2 (a) D. S. Auld and T. Bergman, *Cell. Mol. Life Sci.* 2008, **65**, 3961. (b) M. N. Giles, B. A. Watts, I. G. Giles, H. F. Fry, A. J. Littlechild and C. Jacob, *Chem. & Biol.* 2003, **10**, 677. (c) M. N. Giles, I. G. Giles and C. Jacob, *Biochem. Biophys. Res. Commun.* 2003, **300**, 1.

3 (a) B. S. Sobolov, D. M. Leonida, B. A. Malik, I. K. Voivodov, F. McKinney, J. Kim and J. Fry, *J. Org. Chem.* 1996, **61**, 2125. (b) H. E. Schoemaker, D. Mink and M. G. Wubbolts, *Science* 2003, **299**, 1694. (c) H. Egami and T. Katsuki, *J. Am. Chem. Soc.* 2007, **129**, 8940.

4 (a) M. Landwehr, L. Hochrein, R. C. Otey, A. Kasrayan, E. J. Bäckvall and H. F. Amold, *J. Am. Chem. Soc.* 2006, **128**, 6058. (b) Y. Liou, P. Charoenkwan, Y. S. Srinivasulu, T. Vasylenko, S. Lai, H. Lee, Y. Chen, H. Huang and S. Ho, *BMC Bioinformatics* 2014, **15** (Suppl 16), S4.

5 (a) G. Jepkorir, J. C. Rodríguez, H. Rui, W. Im, S. Lovell, K. P. Battaile, A. Y. Alontaga, E. T. Yukl, P. Moënne-Loccoz and M. Rivera, *J. Am. Chem. Soc.,* 2010, **132**, 9857. (b) S. Ozaki, A. Nakahara and T. Sato, *Chem. Let.* 2011, **40**, 362. (c) S. Ozaki, A. Sato, T. Sato, T. C. Migita, T. Uchida and K. Ishimori, *J. Inorg. Biochem.* 2014, **138**, 31.

6 (a) M. L. Oldham, D. Khare, F. A. Quiocho, A. L. Davidson and J. Chen, *Nature* 2007, **450**, 515. (b) S. Krieg, F. Huche, K. Diederichs, N. Izadi-Pruneyre, A. Lecroisey, C. Wandersman, P. Delepelaire

and W. Welte, *PNAS* 2009, **106(4)**, 1045. (c) N. Izadi-Pruneyre, N. Wolff, V. Redeker, C. Wandersman, M. Delepierre and A. Lecroisey, *J. Bacteriol.* 1999, **261**, 562. (d) F. P. Guengerich, *Chem. Res. Toxicol.* 2001, **14**, 611.

7 (a) O. Shoji, T. Fujishiro, H. Nakajima, M. Kim, S. Nagano, Y. Shiro and Y. Watanabe, *Angew. Chem. Int. Ed*. 2007, **46**, 3656. (b) T. H. Yosca, J. Rittle, C. M. Krest, E. L. Onderko, A.-R. K. Beham and M. T. Green, *Science* 2013, **342**, 825. (c) A-L. Johansson, J. Carlsson, M. Hogbom, J. P. Hosler, R. B. Gennis and P. Brzezinski, *Biochemistry* 2013, **52**, 827.

8 (a) H. Nagaoka and H. Kayahara, *Biosci. Biotechnol. Biochem.* 1999, **63**, 1991. (b) H. Nagaoka and H. Kayahara, *Biosci. Biotechnol. Biochem.* 2000, **64**, 781. (c) H. Nagaoka, H. Kayahara and Y. Wakabayashi, *Biosci. Biotechnol. Biochem.* 2001, **65**, 634.

9 (a) H. Nagaoka, *Biotechnol. Prog.* 2003, **19**, 1149. (b) H. Nagaoka, *Biotechnol. Prog.* 2005, **21**, 405. (c) H. Nagaoka, *Curr. Top. Nutraceutical Res.* 2003, **1**, 281. (d) H. Nagaoka, *Biotechnol. Prog.* 2004, **20**, 128.

10 H. Nagaoka, K. Udagawa and K. Kirimura, *Biotechnol. Prog.* 2012, **28**, 953.

11 V. V. Thakur and A. Sudalai, *Indian. J. Chem.* 2005, **44B**, 557.

12 H. Nagaoka, *RSC Adv.* 2014, **4**, 16333.

13 H. Nagaoka, *ACS Catal.* 2014, **4**, 553.

14 I. T. Paulsen, C. M. Press, J. Ravel, D. Y. Kobayashi, G. S. Myers, D. V. Mavrodi, R. T. DeBoy, R. Seshadri, Q. Ren, R. Madupu, R. J. Dodson, A. S. Durkin, L. M. Brinkac, S. C. Daugherty, S. A. Sullivan, M. J. Rosovitz, M. L. Gwinn, L. Zhou, D. J. Schneider, S. W. Cartinhour, W. C. Nelson, J. Weidman, K. Watkins, K. Tran, H. Khouri, E. A. Pierson, L. S. Pierson 3rd, L. S. Thomashow and J. E. Loper, *Nat. Biotechnol.* 2005, **23**, 873.

15 Ortiz de Montellano, P. R. In *Cytochrome P450*: *Structure, Mechanism, and Biochemistry*, 3rd ed.; Kluwer Academic/Plenum: New York, Boston, Dorcrecht, London, Mosow, 2004.

16 W. Adam, W. Boland, J. Hartmann-Schreier, H-U. Hump, M. Lazarus, A. Saffert, C. R. Saha-Moller and P. Schreier, *J. Am. Chem. Soc.* **1998**, 120, 11044.

17 (a) M. Sakai, H. Futamata, Y. Urashima and T. Matuguchi, *Soil. Sci. Plant Nutr.,* 1995, **41**, 605. (b) S. Sano, T. Sano, I. Morishima, Y. Shiro and Y. Maeda, *Proc. Natl. Acad. Sci. USA*, 1986, **83**, 531.

18 A. R. McDonald, M. R. Bukowski, E. R. Farquhar, T. A. Jackson, K. D. Koehntop, Mi Sook Seo, R. F. De Hont, A. Stubna, J. A. Halfen, E. Muonck, W. Nam and L. Que, Jr. *J. Am. Chem. Soc.* 2010, **132**, 17118.

19 (a) T. Ikeue, Y. Ohgo, T. Yamaguchi, M. Takahashi, M. Takeda and M. Nakamura, *Angew. Chem., Int. Ed.* 2001, **40**, 2617. (b) Y. Ohgo, Y. Chiba, D. Hashizume, H. Uekusa, T. Ozeki and M. Nakamura, *Chem. Commun.*, 2006, **18**, 1935.

20 I. Garcia-Rubio, M. Braun, I. Gromov, L. Thony-Meyer and A. Schweiger, *Biophys. J.* 2007, **92**, 1361

21 S. Radutoiu, L. H. Madsen, E. B. Madsen, H. H. Felle, Y. Umehara, M. Grønlund, S. Sato, Y. Nakamura, S. Tabata, N. Sandal and J. Stougaard, *Nature*, 2003, **425**, 585.

22 H. Hirakawa and T. Nagamune, *ChemBioChem*, 2010, **11**, 1517.

23 (a) M. K. Lam, K. T. Lee, and A. R. Mohamed. *Biotechnol. Adv.* 2010, **28(4)**, 500. (b) Z. Y. Zhao, J. Liu, M. Hahn, S. Qiao, A. P. J. Middelberg, and L. He, *RSC Adv.* 2013, **3**, 22008.

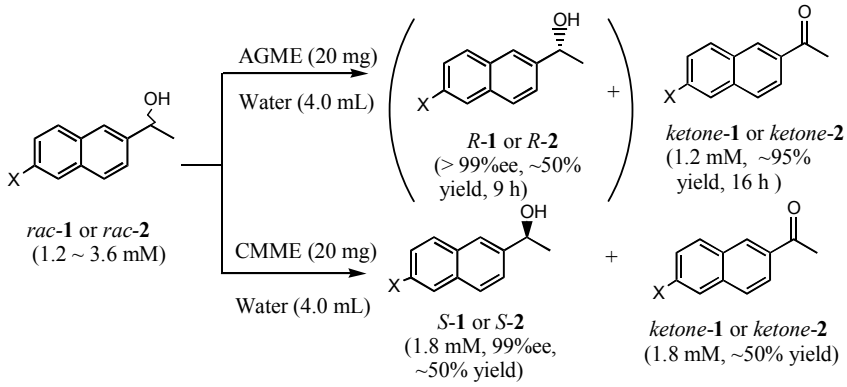

Rac-1: *racemic*-1-(6-methoxynaphthalen-2-yl)ethanol (*S*-naproxen precursor)
Rac-2: *racemic*-1-(2-naphthyl)ethanol
AGME: PEG(MW: 4000/1000 = 1/2)-aggregated ME
CMME: GA-/compound-modified ME
X: -OCH_3(rac-1) -H (rac-2)

[Equation 1]

Figure Captions

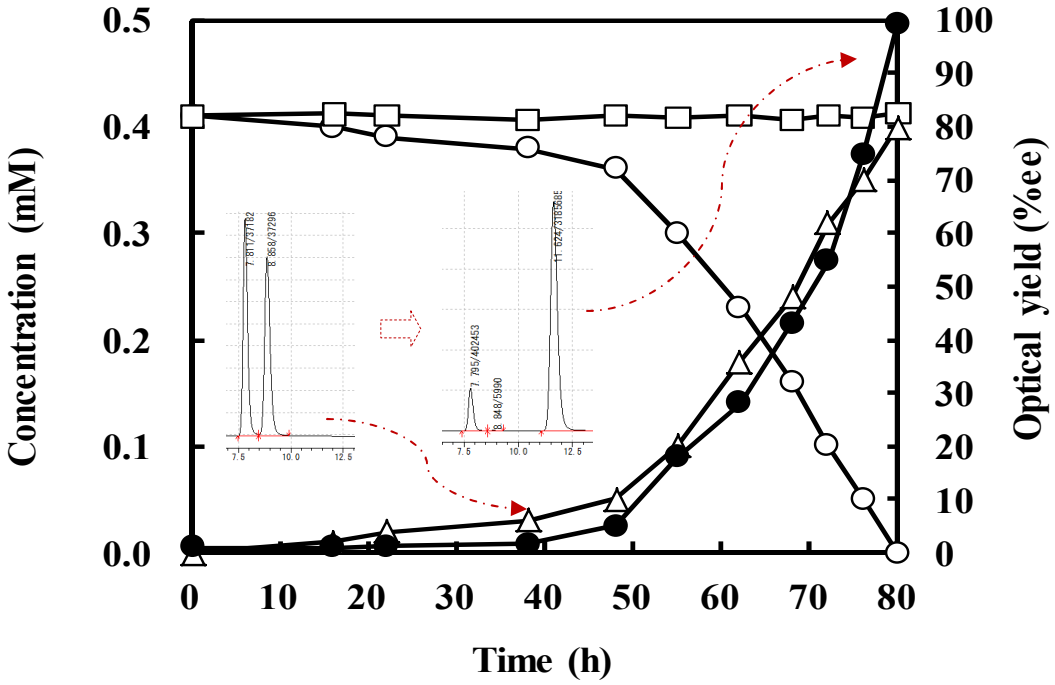

Figure 1. Time course of the asymmetric oxidation activity (-●-: % ee) using an HASApf expressed (20 μM) and substrate *rac*-2 (0.8 mM) in highly bubbled oxygen water as a solvent (5.0 mL), monitoring *S*-2 (-□-: 0.4 mM), *R*-2 (-○-: 0.4 mM), and product ketone (-△-).

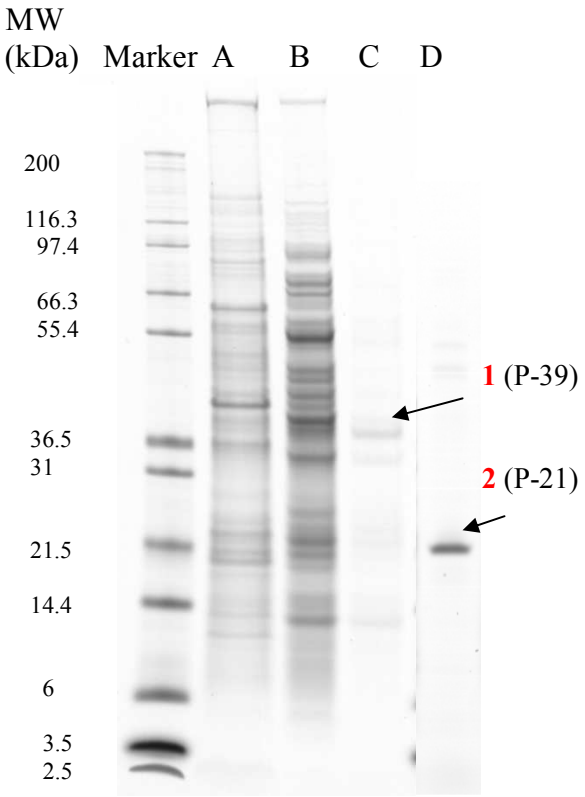

Legend:

There is a separation of a redoxin from PP-HASApf–redoxin complex (**1**); only HASApf appears at 20.8 kDa (**2**) due to hexane extraction after reaction with sample C.

Labelled bands:

1. PP-HASApf-redoxin complex (39 kDa-protein).

2. An HASApf gene product [*Pseudomonas fluorescens* Pf-5] from plant commensal bacteria (20.8 kDa).

Figure 2. SDS-PAGE in four samples: (A) Supernatant 1 (10 µL), (B) Supernatant 2 (10 µL), (C) Supernatant 2 after ultrafiltrating with Vivaspin 2–10 K (10 µL), and (D) Sample C extracted by hexane after reaction (10 µL). Each fraction asymmetrically oxidizes one of the enantiomers in *rac*-2.

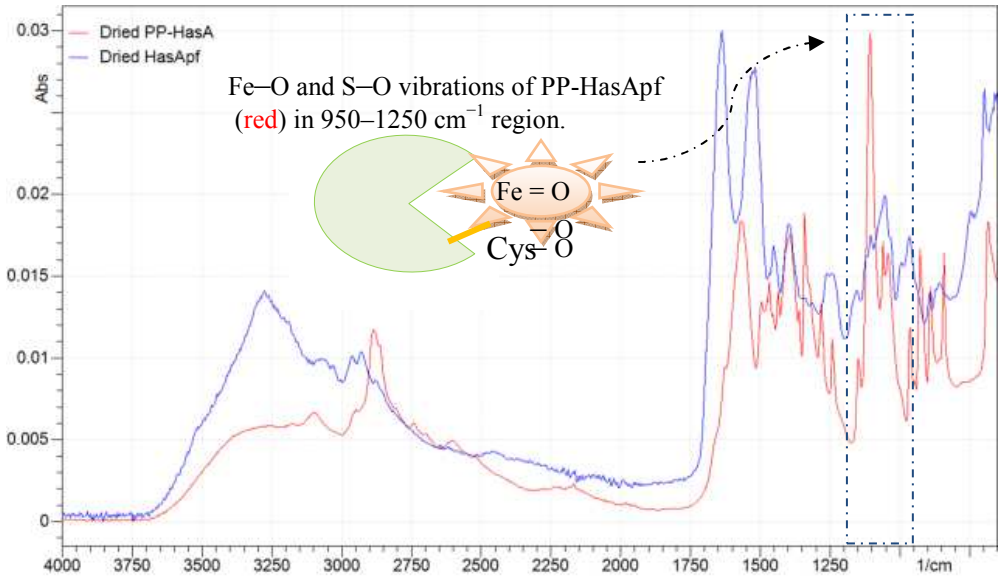

Figure 3. Juxtaposed FTIR spectra of dried HASApf expressed and dried supernatant 2 after

ultrafiltering with Vivaspin 2–10 K. The peak around 950–1250 cm^{-1} may be attributed to the metal-bound sulfinate S–O and Fe–O vibrations ($\nu_s(SO_2) \approx 950–1050\ cm^{-1}$ and $\nu_{as}(SO_2) \approx 1100–1200\ cm^{-1}$).

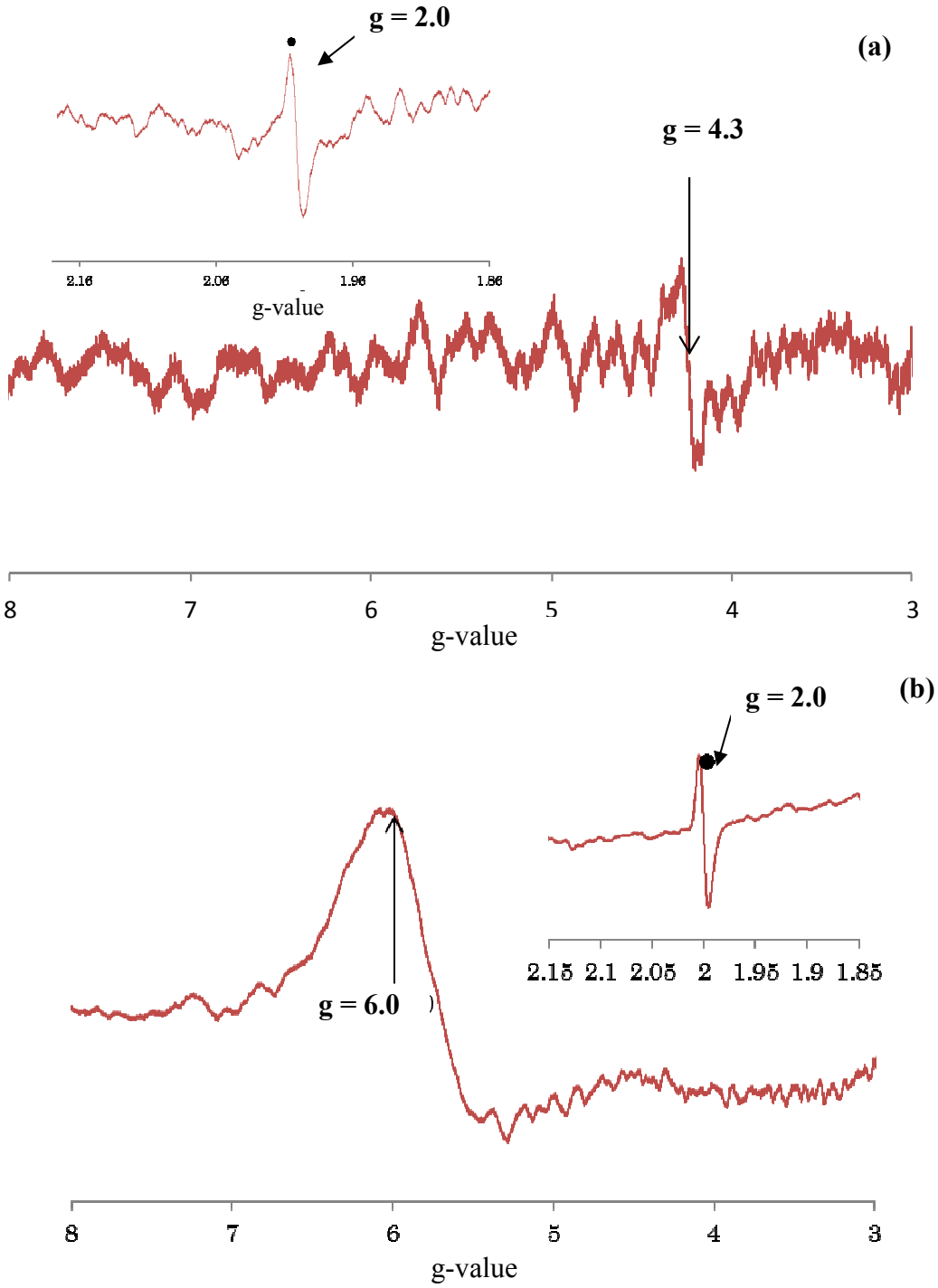

Figure 4. ESR spectroscopy of Fe(III) from (**a**) dried supernatant 2 after ultrafiltrating with Vivaspin 2–10 K and (**b**) dried HASApf expressed: **(a)** two signals appear at g = 4.3 and g = 2.0, suggesting the ferric form (PP-HASApf-ferrodoxin or –rubredoxin complex) or oxoferryl-Fe(IV) = O). **(b)** two signals appear at g = 6.0 and g = 2.0, suggesting the presence of axially symmetric low-spin ferric His/Tyr-heme

iron.

Table 1. IC analysis and ICP-AES (metal) results for dried supernatant 2 and dried HASApf expressed.

Sample	IC (wt%) and ICP-AES (ppm) results						
	C[a]	**H**[a]	**N**[a]	**O**[a]	**S**[a]	**Fe**[b]	**Residues**
Dried Supernatane 2	37.7 ± 0.7	7.3 ± 0.4	8.5 ± 0.7	39 ± 0.2*	0.05 ± 0.01*	3*	-
HasApf dried[c]	83.9	-	1.55	5.60	0.09*	8*	-

C[a]**/H**[a]**/N**[a]**/O**[a]**/S**[a]: The concentrations were measured by IC (elements) analysis (wt%).
Fe[b]: ICP-AES (metal) was performed (ppm).
HasApf dried[c]: Each concentration was measured through both radiation induced X-ray emission and energy dispersive X-ray spectroscopy (Figure 4S).
*Note that whereas iron (Fe) and sulphur (S) in dried supernatant 2 are reduced by half, oxygen appears higher than that of HasApf, suggesting that thesulphate heme (PP-HasApf) is effectively purified.

Table 2. Comparison between the asymmetric oxidation activity of each fraction using a 100 nm oxygen bubble-water as a solvent.

Forms (30 mg)	Product	Reactions (*rac*-**1** or *rac*-**2**)				Minerals[c]	
		Solvent	Time (h)	Unit[d] (mg·min)	Substrate (%)	Ca^{2+} (%)	Fe^{2+} (ppm) (Fe/mol)
Dried Precipitate 1	*S*-1, S-2 ≥99%ee, ~50% CY[a]	D.W.[b]	30	-	-	2.9 ± 0.2	220 ± 5 (≒4 μmol)
		O_2-D.W.[d]	25				
PEG-Precipitate 2 (CMME)	*S*-1, S-2 ≥99%ee, ~50% CY[a]	D.W.[b]	15	0.6 ± 0.02 mU	≥0.06	2.6 ± 0.2	215 ± 5 (≒4 μmol)
		O_2-D.W.[d]	13	0.7 ± 0.02 mU	≥0.06		
AG-Precipitate 2 (AGME)	*R*-1, R-2 ≥99%ee, ~50% CY[b]	D.W.[b]	9	0.8 ± 0.03 mU	≥0.06	2.5 ± 0.2	213 ± 5 (≒4 μmol)
		O_2-D.W.[d]	8				

[a]Chemical yield (%). [b]Distilled water. [c]Mineral values were determined by ICP-AES; Mean ± SD (n = 4).
[d] O_2-D.W. is a highly bubbled oxygen water as a solvent.

Table 3. Results of a BLAST query sequence analysis based on the N-terminal amino-acid sequence identified from Sample D (band 2)

Cycle No. for Sample D (band 2)
N-terminal amino-acid sequence identified (33 residues)

1.	M	S	X[a]	S	I	S	Y	S	T	X[b]	Y	A	T	N	T	V	A	Q	Y	L	X[a]	D	W	X[b]	A	Y	F	G	D	L
30.	N	H	R	E																											

Cycle No. for YP 262445.1[c]
Full length gene and protein sequence based on a BLAST query sequence analysis

1.	M	S	I	S	I	S	Y	S	A	T	Y	G	G	N	T	V	A	G	Y	L	T	D	W	S	A	Y	F	G	D	V
	atg	agc	att	tcg	atc	tct	tac	agc	gct	acc	tac	ggc	ggt	aat	act	gtt	gcg	caa	tac	ctg	act	gac	tgg	tcg	gcc	tac	ttc	ggc	gac	gtc
30.	N	H	R	P	G	E	V	V	D	G	T	N	T	G	G	F	N	P	G	P	F	D	G	T	Q	Y	A	I	K	S
	aac	**cac**	cgc	cca	ggc	gaa	gtg	gtc	gac	ggc	acc	aac	acc	ggt	ggc	ttc	aac	ccg	ggc	ccg	ttc	gac	ggc	acc	cag	tac	gcc	atc	aag	agc
60.	T	A	S	D	A	A	F	V	A	D	G	N	L	H	**Y**	T	L	F	S	N	P	S	**H**	T	L	W	G	S	V	D
	acc	gcc	agt	gac	gcg	gcc	ttc	gtc	gcc	gac	ggc	aac	ctg	cac	**tac**	acc	ctg	ttc	agc	aac	ccg	agc	**cac**	acc	ctg	tgg	ggc	tcg	gtg	gac
90.	T	I	S	L	G	D	T	L	A	G	G	S	G	S	N	Y	N	L	V	S	Q	E	V	S	F	T	N	L	G	L
	act	atc	tcc	ctg	ggc	gac	acc	ctc	gcc	ggt	ggt	tcg	ggc	agc	aac	tac	aac	ctg	gtc	agc	cag	gaa	gtc	agc	ttc	acc	aac	ctg	ggc	ctc
120.	N	S	L	K	E	E	G	R	A	G	E	V	H	K	V	V	Y	G	L	M	S	G	D	S	S	A	L	A	G	E
	aac	agc	ctg	aag	gaa	gaa	ggc	cgt	gca	ggc	gaa	gtg	cac	aag	gtg	gtc	tac	ggc	ctg	atg	agt	ggc	gac	agc	tcg	gcg	ctg	gcc	ggc	gag
150.	I	D	A	L	L	K	A	I	D	P	S	L	S	V	N	S	T	F	D	D	L	A	A	A	G	V	A	H	V	N
	atc	gat	gcc	ctg	ctc	aag	gcg	atc	gac	cca	agc	ctg	tcg	gtg	aac	tcc	acc	ttc	gac	gac	ctg	gcc	gct	gct	ggc	gtt	gct	cac	gtc	aac
180.	P	A	A	A	A	A	A	D	V	G	L	V	G	V	Q	D	V	A	Q	D	W	A	L	A	A					
	ccg	gct	gcc	gca	gcc	gct	gcc	gat	gtt	ggc	ctg	gtg	ggt	gtg	cag	gac	gtg	gcc	cag	gac	tgg	gcg	ctg	gcc	gcc					

Protein sequence on iron–sulfur rubredoxin[15]

1.	M	K	K	Y	T	C	T	V	C	G	Y	I	Y	D	P	E	D	G	D	P	D	D	G	V	N	P	G	T	D	F
30.	K	D	I	P	D	D	W	V	C	P	L	C	G	V	G	K	D	E	F	E	E	V	E	E						

Protein sequence of spinach on iron–sulfur ferredoxin[15]

1.	M	S	H	S	V	K	I	Y	D	T	C	I	G	C	Y	Q	C	V	R	A	C	P	T	D	V	L	E	M	I	P
30.	W	P	G	C	K	A	K	Q	I	A	S	A	P	R	T	E	D	C	V	G	C	K	R	C	E	S	A	C	P	T
60.	D	F	L	S	V	R	V	Y	L	W	H	E	T	T	R	S	M	G	L	A	Y									

X[a]: may be Cys (C) but not detected, X[b]: many amino acids were detected.
[c]YP 262445.1: the accession hit on the query sequence was limited between the query coverage (>93%) and E value (2e-11), a 20.853 Da HasAp gene product [hemophore: *Pseudomonas fluorescens Pf-5*] from plant commensal bacteria, which can inhibit the rhizosphere and produce secondary metabolites that suppress soil-borne plant pathogens.
Red amino acids indicate "hits" between Sample D (band 2) and YP 262445.1[c].
Blue indicates the heme-binding site: His-32 (bearing loop), Tyr-75 (axial heme ligand), and His-83 (hydrogen ligand).
Squares indicate the Cys (C) or Met (M) including sulfur.
Protein sequence based on a BLAST query sequence analysis of Cycle No. for YP 262445.1 is available on NCBI resource: http://www.ncbi.nlm.nih.gov/protein/70732682 and the full length gene sequences on PATRIC: VBIPseFlu72549_5489: http://patricbrc.vbi.vt.edu/portal/portal/patric/Feature?cType=feature&cId=19880237.

a. HasApf (*P. fluorescence*) purification for biocatalytic applications

1. PP → 2. PP gel under aeration → 3. PP gel suspension

Centrifugation (10,000 rpm)

4. **Supernatant 1** & 5. **Preciptate 1** → FD { 5a. **Dried Precipitate 1**: no treatment with a buffer

Precipitate 1 dissolved by 1.0%PEG(1000/4000 or 4000)/50 mM glycineNaOH (and GE) solution

Centrifugation (10,000 rpm)

6. **Preciptate 2** & 7. **Supernatant 2** → ultrafiltrating with Vivaspin 2–10 K → FD

FD { **Dried Preciptate 2**: treatment with a buffer

{ 6a. **AG-Precipitate 2 (AGME)**: a buffer/PEG (MW: 1000/4000)/GE → FD
6b. **CM-Precipitate 2 (CMME)**: a buffer/GA and PEG (4000)/GE → FD

b. Relation of the amount of bacteria to the kinetic resolutions of *rac* -2 for each fraction.

Process (each fraction)		Materials	Bacteria (CFU/g)		Resolutions			Outcomes
					rac-2/ catalyst	Times	Result	
1	PP	powder	210[f]	Detected types: 1. aerobic spore-bearing bacterium (*Geobacillus, Alicyclobacillus, Bacillus, Paenibacillus*) 2. catalase-and gram-positive coccus bacterium (*Staphylococcus, Kocuria, Micrococcus*)				
2	PP gel under aeration	Na^+alginate	ND[a]					
		$Ca^{2+}Cl_2$						
		D.W.						
		PP gel	∞					
3	PP gel suspension	solution			1.2 mM/5 mL[b]	10 h	N.R.[d]	PP-HASApf weakly actvated!
4	Supernatant 1	solution						
5a	Precipitate 1 dried	powder	ND[a]		1.2 mM/30 mg[c]	15 h	C.R.[e]	PP-HASApf highly activated by buffered glycin!
6	Precipitate 2 dried	powder						
6a	AG-Precipitate 2	powder						
6b	PEG-Precipitate 2	powder						
7	Supernatant 2	solution	∞		1.2 mM/5 mL[b]	10 h		

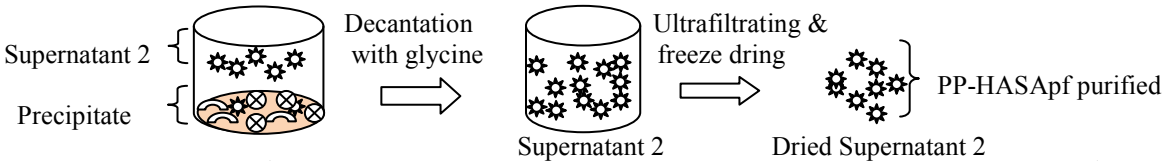

ND[a] = not detected. 0.8 mM/5 mL[b] = solvent is detected as is. 1.2 mM/30 mg[c] = adding D.W. (5 mL). N.R.[d] = not completely resolved. C.R.[e] = completely resolved. 210[f] = in the test of Serial Analysis of Gene Expression, *P. fluorescence* PF-5 is not detected except the two types.

Scheme 1. (**a**) Purification flow of a PP-HASApf-redoxin complex eluted from PP gel under aeration and (**b**) its application to the catalysis of enantioselective oxidation in organic synthesis.